JOURNAL OF PROPULSION AND POWER
Vol. 26, No. 3, May–June 2010

Ultrasonic Signal Denoising for Robust Measurement of Solid-Propellant Burning Rates

Su-Kyun Jeon,* Sung-Jin Song,† Hak-Joon Kim,‡ Sun-Feel Ko,§ and Hyun-Taek Oh¶
Sungkyunkwan University, Suwon, 440-746 Republic of Korea
and
In-Chul Kim,** Ji-Chang Yoo,†† and Jung Yong Jung‡‡
Agency for Defense Development, Daejeon, 305-152 Republic of Korea

DOI: 10.2514/1.45575

Recently, an effective approach (namely, an ultrasonic full-waveform analysis method) has been proposed for the ultrasonic measurement of solid-propellant burning rate as a function of pressure in a single test. In this study, high-frequency ultrasonic transducers are adopted for the acquisition of ultrasonic full waveforms in order to increase the spatial resolution of the measurement. Unfortunately, however, these transducers are susceptible to random noise. This paper addresses an effective approach for reducing high-frequency random noise to the ultrasonic full waveforms using the wavelet-shrinkage method. Furthermore, this paper presents the results of the noise reduction at ultrasonic full waveforms captured from solid-propellant samples together with the improvement in the measurement accuracy of solid-propellant burning rates obtained by adopting the proposed approach.

Nomenclature

e	=	Gaussian white noise
h_L, g_L	=	Daubechies's sequence
j	=	resolution level
j_L	=	level of orthogonal wavelet transform
L	=	length of the signal
L_D	=	length of the Daubechies's sequence
L_j	=	length of the wavelet coefficient at level j
s	=	scaling coefficient
u	=	original signal
w	=	wavelet coefficient
w_e	=	wavelet coefficient of Gaussian white noise
w_u	=	wavelet coefficient of original signal
w_x	=	wavelet coefficient of observed signal
w_xN	=	wavelet coefficient after soft-thresholding
x	=	observed signal
λ	=	threshold level
σ	=	standard deviation
$\hat{\sigma}$	=	estimated standard deviation

I. Introduction

ULTRASONIC techniques have been adopted for many years for measuring burning rates of a solid propellant as a function of pressure, since they have a very unique advantage of determining the burning rates in a wide range of pressure in only a single test [1]. Even though there are some variations in detail configurations of measuring systems, the basic setup for measurement of solid-propellant burning rates using ultrasound is quite similar.

Figure 1 schematically shows a typical measurement setup, in which a solid-propellant sample is inserted in a combustion bomb (which is often called a closed bomb) while attached to a solid couplant. A normal beam ultrasonic transducer is contacted to the solid couplant from outside of the combustion bomb so that it can be protected from heat and pressure produced by propellant burning. Obviously, the length of the solid propellant decreases during propellant burning, while the pressure inside the closed bomb increases due to gases produced by propellant burning. In this measurement setup, the length of the burning propellant is measured by the attached ultrasonic transducer, and the pressure inside the closed bomb is monitored by the attached pressure sensor (as shown in Fig. 1). The burning rates of most propellants vary according to the pressure, so it is necessary to measure the burning rate of a solid propellant as a function of pressure. This task can be completed rather easily by measuring the instantaneous length of the propellant sample and the pressure inside the closed bomb simultaneously. In fact, this allows the determination of burning rate versus pressure. Furthermore, by having this simultaneous measurement (with a sufficiently high rate) over an entire period of propellant burning, one can determine the solid-propellant burning rate as a function of pressure in a single burning test using only one propellant sample.

Even though the basic principle of ultrasonic measurement of solid-propellant burning rate is quite simple, as mentioned above, for the determinations of detail configuration of test setup, measurement procedure, and implementation of data analysis algorithm, however, one should address properly following key issues: 1) simultaneous acquisition of ultrasonic signal and pressure data at a sufficiently high rate, 2) ultrasonic wave-speed variation with pressure, and 3) high attenuation of ultrasound in solid-propellant samples.

In fact, careful consideration of all these issues together had resulted in ultrasonic measurement setups in which the arrival time of an ultrasonic signal peak was detected at a very high speed (about 2000 times per second) using the dedicated hardware circuits [2,3]. However, using these peak-detection systems required three different tests in series: 1) the pretest (before the burning test) to investigate the wave-speed variations in the propellant and the couplant, 2) the burning test to measure the burning rate of solid propellant with actual burning, and 3) the posttest (with couplant only after the burning test) to determine the wave-speed variation in the solid couplant. From the pretest and the posttest, the ultrasonic wave speed of the solid propellant was determined as a function pressure, and then instantaneous length of the propellant is determined first. Then the

Received 13 July 2009; revision received 16 November 2009; accepted for publication 11 January 2010.

*Postdoctoral Student, School of Mechanical Engineering; jsk4544@skku.edu.
†Professor, School of Mechanical Engineering; sjsong@skku.edu. Member AIAA.
‡Research Professor, School of Mechanical Engineering; hjkim21c@skku.edu.
§Researcher, School of Mechanical Engineering; madboy@naver.com.
¶Ph.D. Student, School of Mechanical Engineering; liefellen@skku.edu.
**Researcher, Core Technology Development; kic5600@hanmail.net.
††Researcher, Core Technology Development; yoojic@hanmail.net.
‡‡Researcher, Core Technology Development; jjw1351@hanmail.net.

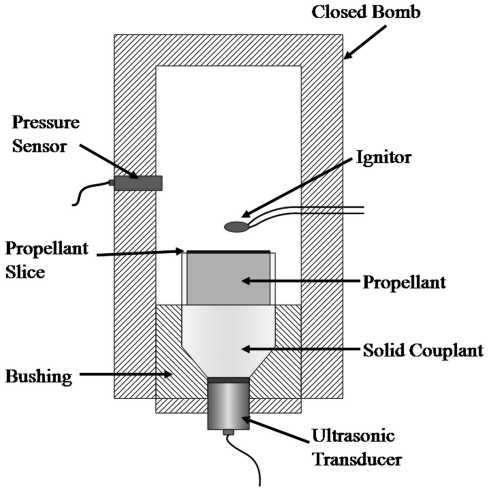

Fig. 1 A schematic representation of ultrasonic testing setup for measuring burning rates of a solid-propellant sample mounted in a closed bomb.

burning rates of the solid propellant at various pressure levels were determined. Since the posttest had to be performed when the temperature of the solid couplant dropped down to the temperature at which the pretest was performed, it was usually performed about 2 h after the end of the burning test. These approaches were very time- and cost-consuming and were easily contaminated by various sources of error [4].

Recently, more effective approaches [5–8] were proposed in which full waveforms of ultrasonic signals were acquired and analyzed at high enough speed by taking advantages of modern digital signal-processing technology. In these approaches, up to 2000 ultrasonic full waveforms were acquired and digitized in a second and then stored in the memory of the measurement system for postprocessing to be made later. Therefore, these approaches can be considered as the full-waveform analysis method. The most outstanding feature of the full-waveform analysis approach is the elimination of the posttesting that made the conventional peak-detection approaches time- and cost-consuming. Therefore, the new approach is very efficient in terms of time and cost.

In this efficient approach, the ultrasonic wave speeds of solid propellant at various pressures are determined from the pretest. For this purpose, ultrasonic full waveforms are acquired at various pressures together with the corresponding pressure. Figure 2 shows examples of such measurements. As shown in Fig. 2, there are two distinct signal groups in the acquired ultrasonic waveforms: 1) the interface echo, which is the reflected wave from the interface between the solid propellant and the solid couplant, and 2) the surface echo reflected at the end of the solid propellant. The decrease of the arrival time of the interface echo (with increasing pressure) is due to the wave-speed increase in the solid couplant, while that of the surface echo is due to the wave-speed changes in the solid couplant and the solid propellant. Therefore, the change in the time of flight (TOF) between these two echoes is produced by the wave-speed variation in the solid couplant only. Here, obviously, it is assumed that the lengths of both the solid couplant and the solid propellant do not vary during the pretest, which was confirmed by the actual observation. Since the full waveforms are stored in a digitized data format, the TOF between the interface and the surface echoes can be determined by adopting various algorithms such as cross-correlation [9]. Once the TOF value is determined at a certain pressure level, the wave speed at that pressure is estimated by simple division of the TOF value by twice the original length of the solid-propellant sample.

In the burning test, similar waveforms are also acquired together with corresponding pressure data for an entire period of propellant burning. Figure 3 shows examples of such measurements, where one can see the gradual decrease of TOF values between the two echoes as the increase of pressure inside the closed bomb. Therefore, if one measures the TOF values for a certain pressure and multiplies by twice the wave speed at that pressure value (which is already determined in the pretest), then one can determine the instantaneous length of the solid propellant while burning. In the burning test, a series of waveforms and pressure values are acquired continuously at a high enough rate so that differentiation of the instantaneous length of the solid propellant with respect to time can be performed to determine the burning rate of the solid propellant at the interrogated pressure level.

Another important feature of the full-waveform analysis approach is use of a high-frequency transducer. Considering the fact that solid propellants are materials with high attenuation to ultrasound, in the conventional peak-detection approaches, relatively low-frequency transducers (with center frequency of 1 MHz) have been most frequently adopted. However, in the full-waveform analysis approach, high-frequency ultrasound is more suitable, since it shows better resolution in time, which is a desired property for the description of full waveforms in detail.

Therefore, the full-waveform analysis approach adopts ultrasonic transducers with 5 MHz center frequency. In fact, the ultrasonic signals shown in Figs. 2 and 3 were also acquired by the 5 MHz ultrasonic transducers.

However, high-frequency transducers have a drawback, which is that they are more easily affected by noise. In fact, there are three random-noise sources in the ultrasonic measurement of the burning rates of solid propellants: 1) electric random noise that can contaminate ultrasonic signals, 2) noise produced from the solid propellant itself, which is composed of numerous tiny grains oriented randomly, and 3) noise generated from the burning surface, which is assumed to remain perfectly flat during propellant burning, but actually has random roughness in real burning surfaces so that it can also produce the random fluctuation in the surface echo [10]. These three types of random noises are higher in frequency compared with the two signal echoes (the interface echo and the surface echo),

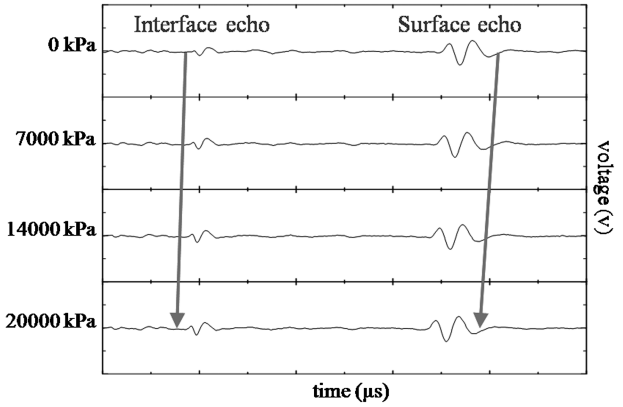

Fig. 2 Ultrasonic waveforms acquired during the pretest result of a solid propellant.

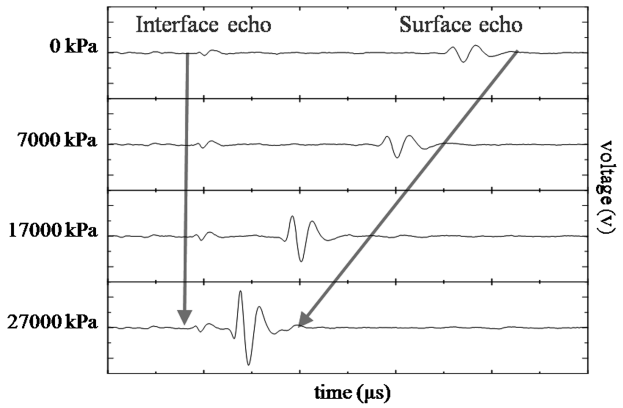

Fig. 3 Ultrasonic waveforms acquired during the burning test of a solid propellant.

which have the frequency components of around 600 kHz. Even though the amplitudes of these high-frequency noises are not big compared with those of the echoes, they can certainly affect the measurement of TOF values, since the TOF measurement is usually made in an automated fashion using specially developed application software. Considering the fact that the measurement of TOF values in both the pretest and the burning test play a very crucial role, it is therefore strongly desired to reduce these high-frequency random noises in the acquired ultrasonic full waveforms for the reliable and robust measurement of the TOF values.

This paper addresses the reduction of these high-frequency random noise to the ultrasonic full waveforms using the wavelet-shrinkage method [11] that has been proposed for the removal of Gaussian white noise. In the following sections, the wavelet-shrinkage method is briefly addressed first, and then the results of denoising of ultrasonic signals are discussed and the improvements obtained both in the TOF measurement and in the solid-propellant burning-rate determination are presented.

II. Noise Reduction by Wavelet Shrinkage

Various filters have been proposed until now for the removal of white noise included in a signal. Recently, filtering techniques based on the wavelet transform have been proposed for removing various noises that were difficult to cancel by using frequency-domain filters. For example, a wavelet-domain filtering technique for removing white noise with the edge of the signal preserved is proposed [12].

The wavelet-shrinkage approach can be found in various references, including [13]. However, for the continuity of our discussion, it would be worthwhile here to briefly describe three key ingredients of this approach: 1) the resolution of signal, 2) the reconstruction of signal, and 3) soft-thresholding. An approach for resolving signals using the two scale relations is briefly discussed first. The two scale relations are the relation between the scaling function of level j and the scaling function of level $j-1$ and the relation between the wavelet function of level j and the scaling function of level $j-1$. They can be given by Eqs. (1) and (2):

$$s^{(j)}(k) = \sum_L \bar{h}_L s^{(j-1)}(2k+L) \tag{1}$$

$$w^{(j)}(k) = \sum_L \bar{g}_L s^{(j-1)}(2k+L) \tag{2}$$

Here, $s^{(j)}(k)$ and $w^{(j)}(k)$ are scaling coefficients of the low-frequency element and wavelet coefficients of the high-frequency element, respectively, and L is the length of the signal. In this study, h_L uses Daubechies's sequence of the length $L_D = 4$, as shown in Table 1 [14].

Table 1 Daubechies's sequence [14]

L_D				
2	3	4	6	8
		h_L		
0.4829	0.3326	0.2303	0.1115	0.0544
0.8365	0.8068	0.7148	0.4946	0.3128
0.2241	0.4598	0.6308	0.7511	0.6756
−0.1294	−0.1350	−0.0279	0.3152	0.5853
——	−0.0854	−0.1870	−0.2262	−0.0158
——	0.0352	0.0308	−0.1297	−0.2840
——	——	0.0328	0.0975	0.0004
——	——	−0.0105	0.0275	0.1287
——	——	——	−0.0315	−0.0173
——	——	——	0.0005	−0.0440
——	——	——	0.0047	0.0139
——	——	——	−0.0010	0.0087
——	——	——	——	−0.0048
——	——	——	——	−0.0003
——	——	——	——	0.0006
——	——	——	——	−0.0001

The sequence g_L is decided by Eq. (3):

$$g_L = (-1)^L h_{1-L} \tag{3}$$

The scaling coefficient $s^{(0)}(k)$ of level 0 can be divided into the scaling coefficient $s^{(1)}(k)$ of low accuracy and the wavelet coefficient $w^{(1)}(k)$ by using Eqs. (1) and (2). In general, the low-frequency element of the signal appears in $s^{(j)}(k)$, and the high-frequency element appears in $w^{(j)}(k)$. Figure 4 schematically shows the resolution of the signal into successions scaling coefficients $s^{(j)}(k)$ and the wavelet coefficients $w^{(j)}(k)$.

Specifically, the signal $f(x)$ is resolved into lower-frequency element $s^{(1)}(k)$ and higher-frequency element $w^{(1)}(k)$ by using the orthogonal wavelet transform. This lower-frequency element $s^{(1)}(k)$ is resolved into lower-frequency element $s^{(2)}(k)$ and higher-frequency element $w^{(2)}(k)$. Here, it is worthwhile to note that the lengths of signals $s^{(2)}(k)$ and $w^{(2)}(k)$ are only half of the length of signal $s^{(1)}(k)$. The repetition of this operation to level j is called the *orthogonal wavelet transform*.

The second ingredient is the reconstruction of signal using the wavelet transform. In fact, the signal is reconstructed by using the scaling coefficient and wavelet coefficients according to the following process. At first, the scaling coefficient $s^{(j-1)}(k)$ of level $j-1$ can be given by Eq. (4):

$$s^{(j-1)}(k) = s^{(j)}(k) + w^{(j)}(k) \tag{4}$$

The scaling coefficient of high accuracy can be obtained by using this reconstruction formula. The process for the reconstruction of the signal is shown in Fig. 5.

The third ingredient is soft-thresholding at wavelet coefficients. Recently, Donoho [11] proposed a method, which is called wavelet shrinkage, for reconstructing an unknown function from noisy data. In the wavelet-shrinkage method, the noise included in the signal is removed by the following procedures. Let $u(i)$ be a discrete time original signal and let $e(i)$ be a Gaussian white noise. Then the observed signal $x(i)$ can be written as Eq. (5):

$$x(i) = u(i) + e(i) \qquad (i = 0, 1, \ldots, L-1) \tag{5}$$

Here, L is a length of the signal.

Computing a level j_L orthogonal wavelet transform of the observed signal $x(i)$, the wavelet coefficient $w_x^{(j)}(k)$ is given by Eq. (6):

$$w_x^{(j)}(k) = w_u^{(j)}(k) + w_e^{(j)}(k)$$
$$(j = 1, \ldots, j_L;\ k = 0, 1, \ldots, L_j - 1) \tag{6}$$

Here, L_j is a length of the wavelet coefficient at level j. After the orthogonal wavelet transform, the white noise has the same statistical properties as the untransformed signal. Therefore, the wavelet coefficients $w_e^{(j)}(k)$ of the white noise become white noise. On the other hand, when the original signal $u(i)$ does not contain high-frequency component, the coefficients $w_u^{(j)}(k)$ become 0. Then the white noise can be removed by eliminating the coefficient $w_x^{(j)}(k)$

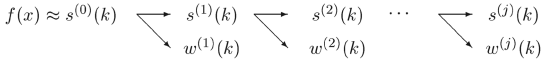

Fig. 4 Resolution of the signal.

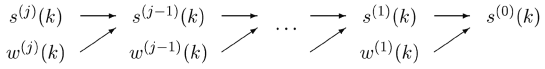

Fig. 5 Reconstruction of the signal.

below a threshold level λ. For the thresholding, Donoho [11] has proposed the following criterion:

$$w_x N^{(j)}(k) = \begin{cases} w_x^{(j)}(k) - \lambda & (w_x^{(j)}(k) > \lambda) \\ 0 & (|w_x^{(j)}(k)| \le \lambda) \\ w_x^{(j)}(k) + \lambda & (w_x^{(j)}(k) < \lambda) \end{cases} \quad (7)$$

This method is called *soft-thresholding*. If the standard deviation σ of the Gaussian noise is already known, the threshold level λ can be determined by Eq. (8):

$$\lambda = \sigma\sqrt{2\log L} \quad (8)$$

If the standard deviation σ of the noise is unknown, the standard deviation can be estimated based on the median absolute deviation. The estimated standard deviation $\hat{\sigma}$ can be calculated by Eq. (9):

$$\hat{\sigma} = \frac{\text{median}\{|w_x^{(1)}(0)|, |w_x^{(1)}(1)|, \ldots, |w_x^{(1)}(L_1 - 1)|\}}{0.6745} \quad (9)$$

The threshold level λ is determined by using the estimated standard deviation $\hat{\sigma}$. Noise reduction is completed by reconstructing the signal by using the coefficient $w_x N^{(j)}(k)$ processed by Eq. (7).

III. Measurement of the Times of Flight and the Burning Rates

The ultrasonic full-waveform analysis approach that has been discussed in the previous section is applied to the solid propellant, which is a composite ammonium-perchlorate/aluminum (AP/Al) propellant. For the measurement, solid-propellant samples were prepared to have both a web thickness and diameter of 20 mm, as shown in Fig. 6. Figure 7 shows an ultrasonic full waveform that has been captured by a 5 MHz ultrasonic transducer during the burning test of the solid propellant. As shown in Fig. 7, the ultrasonic signal was contaminated by high-frequency random noise, which makes the time-of-flight measurement in an automated fashion a truly difficult task. Therefore, the wavelet-shrinkage approach discussed in the last section has been applied to reduce the random noise at the ultrasonic signal shown in Fig. 7.

Figure 8 shows a result of the resolution of ultrasonic full waveform (Fig. 7) using wavelet transformation to the level of $j = 3$. From this figure, it can be noted that the wavelet coefficients (as shown in Figs. 8a–8c) contain the high-frequency random-noise components, and the scaling coefficient (as shown in Fig. 8d) shows the overall variation of the captured signal. Then the soft-thresholding method was applied to the wavelet coefficients (shown in Figs. 8a–8c), and the results are presented in Fig. 9. Comparing Figs. 8 and 9, it is clear that a Gaussian white-noise-included signal in wavelet coefficients has been removed by the soft-thresholding.

Fig. 6 Solid-propellant specimen of AP/Al propellant.

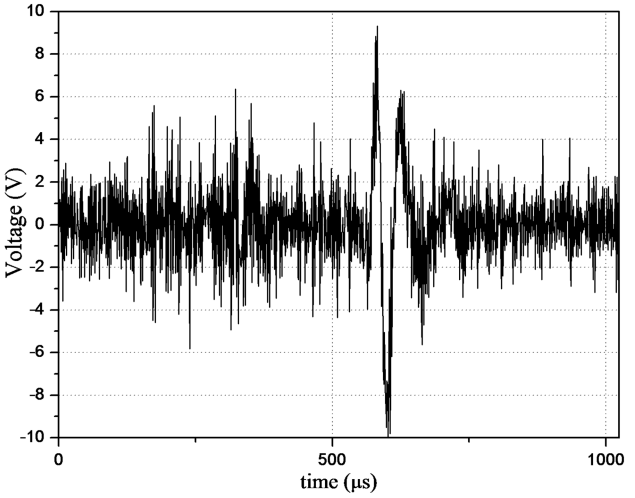

Fig. 7 An example of an ultrasonic full waveform.

By using the scaling coefficient $s^{(3)}(k)$ shown in Fig. 8d and the wavelet coefficients soft-thresholded $w^{(j)}(k)(1 \le j \le 3)$ shown in Fig. 9, the filtered ultrasonic full waveform can be reconstructed. The final reconstructed result is shown in Fig. 10. Comparing Figs. 7 and 10, one can see that the high-frequency random noises have been successfully removed by the wavelet shrinkage.

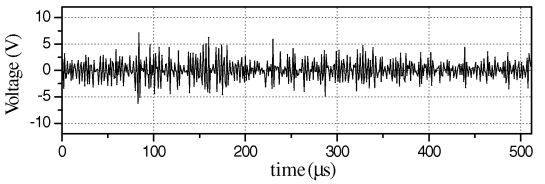

a) Wavelet coefficient at level $j = 1$

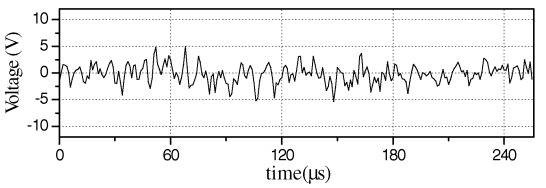

b) Wavelet coefficient at level $j = 2$

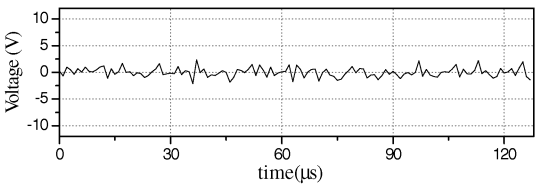

c) Wavelet coefficient at level $j = 3$

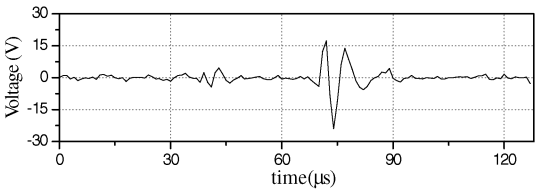

d) Scaling coefficient $s^{(3)}(k)$ of the ultrasonic full waveform

Fig. 8 Resolution of the ultrasonic full waveform.

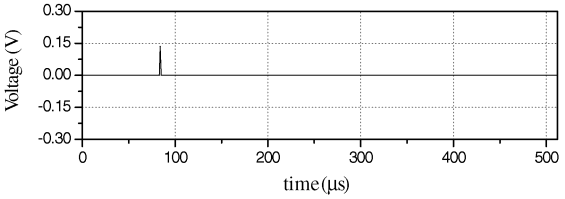

a) Wavelet coefficient at level $j = 1$

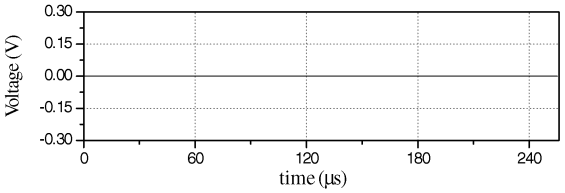

b) Wavelet coefficient at level $j = 2$

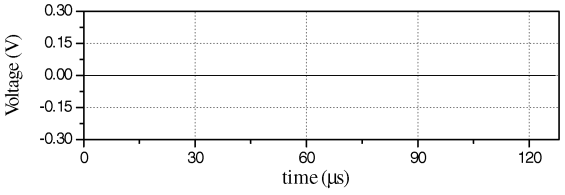

c) Wavelet coefficient at level $j = 3$

Fig. 9 Wavelet coefficients after soft-thresholding.

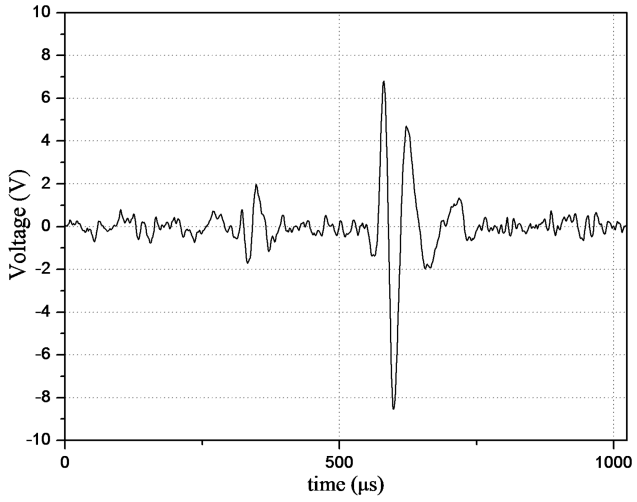

Fig. 10 Reconstruction of the ultrasonic full waveform.

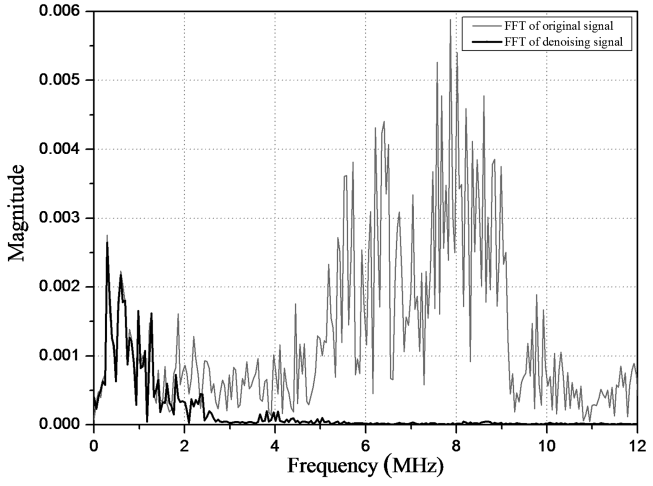

Fig. 11 Frequency spectra of the original signal and the noise-reduced signal.

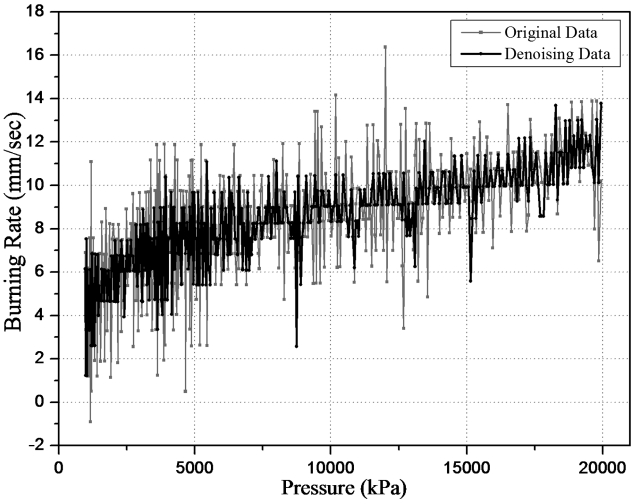

Fig. 12 Comparison of burning-rate measurement results for the solid propellant.

The suppression of high-frequency random noise can be more clearly confirmed from the comparison of frequency spectra of two waveforms, as shown in Fig. 11. The gray line is the frequency spectrum of original ultrasonic full waveform, and the black line is

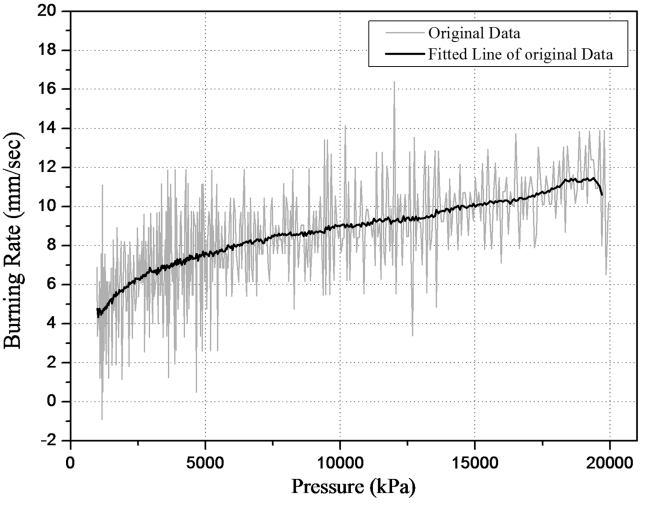

a) Original signal

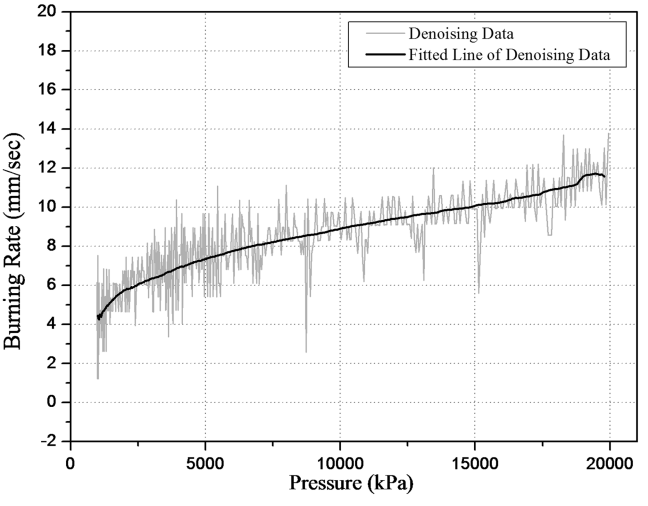

b) Denoised signal

Fig. 13 Spline-curve-fitting results to the measured burning rates.

Table 2 MSE of the specimens

MSE experiment	Noise-included burning rate	Noise-reduced burning rate
Specimen 1	4.10	2.68
Specimen 2	4.80	1.58
Specimen 3	1.10	0.32
Specimen 4	1.79	0.43

that of the denoised waveform. From this figure, one can see the effectiveness of the proposed noise-reduction method very clearly.

The proposed noise-reduction method has been applied to all of the ultrasonic full waveforms captured in the pretest and the burning test. Then the times of flight between the interface echo and the surface echo were measured automatically by specially developed application software in which a cross-correlation analysis had been implemented.

Figure 12 shows the comparison of the burning-rate measurements that have been made to the propellant. In this figure, the gray line shows the measured burning rate from the original signal (Fig. 7), and the black line presents that measured form the noise-reduced signal (Fig. 10). From this result, one can note that the burning-rate measurement made to the denoised signal has much lower fluctuation, compared with the original signal case. However, the burning-rate measurement results (shown in Fig. 12) are discrete in pressure and heavily contaminated by various sources of error, especially including the one related to numerical differentiation. Therefore, it is necessary to carry out proper a data-smoothing operation. One of the efficient ways of data-smoothing that can be applied in this case is the spline-curve-fitting [8]. Figure 13 shows the result of the curve-fitted to burning-rate data.

As shown in this figure, the curve-fitted lines successfully represent the overall behavior of the measured discrete burning-rate data. To demonstrate the effectiveness of the proposed denoising approach, Table 2 shows the mean square errors (MSEs) of the curve-fitted lines for four different propellant specimens. From this table, one can note that the proposed noise-reduction method reduces the MSE values significantly for all four specimens, which means that the proposed denoising approach improved the accuracy of the burning-rate measurement.

IV. Conclusions

Recently, the ultrasonic full-waveform analysis method has been proposed for the ultrasonic measurement of solid-propellant burning rate as a function of pressure in a single test. In this study, high-frequency ultrasonic transducers with a center frequency of 5 MHz are adopted for the acquisition of ultrasonic full waveforms in order to increase the spatial resolution of the measurement. Unfortunately, however, these transducers are susceptible to random noise. This paper addresses an effective approach for reducing high-frequency random noise to the ultrasonic full waveforms using the wavelet-shrinkage method.

Specifically, this paper discussed three key ingredients of the wavelet shrinkage: the resolution of signal, the reconstruction of signal, and the soft-thresholding. In the present study, the proposed approach has been applied to the ultrasonic full waveforms captured during the pretest and the burning test of the solid-propellant samples. The results presented in this paper demonstrate that the high-frequency random noises have been successfully removed by the proposed approach. Furthermore, the MSE values of the spline-curve-fitted data for four different solid-propellant specimens decreased, so one can conclude that the proposed denoising approach improved the accuracy of the burning-rate measurement significantly. The promising results obtained in the present study demonstrate the high potential and capability of the proposed approach.

Acknowledgments

The authors would like to thank the Defense Acquisition Program Administration and the Agency for Defense Development for the financial support provided by both institutions.

References

[1] Frederick, R. A., Jr., Traineau, J. C., and Popo, M., "Review of Ultrasonic Technique for Steady State Burning Rate Measurements," *36th AIAA/ASME/SAE/ASEE Joint Propulsion Conference and Exhibit*, AIAA, Reston, VA, 2000, pp. 2000–3801.

[2] McQuade, W. W., Dauch, F., Moser, M. D., and Frederick, R. A., Jr., "Determination of the Ultrasonic Burning Rate Technique Resolution," *34th AIAA/ASME/SAE/ASEE Joint Propulsion Conference and Exhibit*, AIAA, Reston, VA, 1998, pp. 1998–3555.

[3] Salvo, R. Di., Frederick, R. A., Jr., and Moser, M. D., "Direct Ultrasonic Measurement of Solid Propellant Combustion Transients," *35th AIAA/ASME/SAE/ASEE Joint Propulsion Conference and Exhibit*, AIAA, Reston, VA, 1999, pp. 1999–2223.

[4] Dauch, F. T., "Uncertainty Analysis of the Ultrasonic Technique Applied to Solid Propellant Burning Rate Measurement," M.S. in engineering, Mechanical and Aerospace Engineering Dept., Univ. of Alabama in Huntsville, Huntsville, AL, 1999.

[5] Murphy, J. J., and Krier, H., "Evaluation of Ultrasound Technique for Solid-Propellant Burning-Rate Response Measurements," *Journal of Propulsion and Power*, Vol. 18, No. 3, 2002, pp. 641–651. doi:10.2514/2.5978

[6] Hafenrichter, T. J., Murphy, J. J., and Krier, H., "Ultrasonic Measurement of the Pressure-Coupled Response Function for Composite Solid Propellants," *Journal of Propulsion and Power*, Vol. 20, No. 1, 2004, pp. 110–119. doi:10.2514/1.9237

[7] Song, S. J., Jeon, J. H., Kim, H. J., Kim, I. C., Yoo, J. C., and Jung, J. Y., "Burning Rate Measurement of Solid Propellant Using Ultrasound—Approach and Initial Experiments," *Review of Progress in Quantitative Nondestructive Evaluation*, Vol. 25B, American Inst. of Physics, Melville, NY, 2006, pp. 1229–1236.

[8] Song, S. J., Kim, H. J., Ko, S. F., Oh, H. T., Kim, I. C., Yoo, J. C., and Jung, J. Y., "Measurement of Solid Propellant Burning Rates by Analysis of Ultrasonic Full Waveforms," *Journal of Mechanical Science and Technology*, Vol. 23, No. 4, 2009, pp. 1112–1117. doi:10.1007/s12206-009-0302-y

[9] Jeon, J. H., "A Study on the Burning Rate Measurement of Solid Propellants Using Ultrasonic Technique," M.S. Dissertation, Mechanical Engineering Dept., Sungkyunkwan Univ., Suwon, ROK, 2005.

[10] Song, S. J., Kim, H. J., Oh, H. T., Lee, S. W., Song, S. H., Kim, I. C., Yoo, J. C., and Jung, J. Y., "An Ultrasonic Measurement Model to Predict a Reflected Signal from Non-Liner Burning Surface of Solid Propellants," *Journal of the Korean Society for Nondestructive Testing*, Vol. 27, No. 6, 2007, pp. 531–540.

[11] Donoho, D. L., "De-Noising By Soft-Thresholding," *IEEE Transactions on Information Theory*, Vol. 41, No. 3, 1995, pp. 613–627. doi:10.1109/18.382009

[12] Xu, Y., Weaver, J. B., Healy, D. M. Jr., and Lu, J., "Wavelet Transform Domain Filters: A Spatially Selective Noise Filtration Technique," *IEEE Transactions on Image Processing*, Vol. 3, No. 6, 1994, pp. 747–758. doi:10.1109/83.336245

[13] Ma, J., "Towards Artifact-Free Characterization of Surface Topography Using Complex Wavelets and Total Variation Minimization," *Applied Mathematics and Computation*, Vol. 170, No. 2, 2005, pp. 1014–1030. doi:10.1016/j.amc.2004.12.053

[14] Daubechies, I., *Ten Lectures on Wavelets*, Society for Industrial and Applied Mathematics, Philadelphia, 1992, pp. 194–202.

S. Son
Associate Editor